Proceedings of the 9th International Symposium on
Dynamics and Control of Process Systems (DYCOPS 2010),
Leuven, Belgium, July 5-7, 2010
Mayuresh Kothare, Moses Tade, Alain Vande Wouwer, Ilse Smets (Eds.)

Control of PM10 concentrations over a regional domain

C. Carnevale* V. Filisina G. Finzi E. Pisoni M. Volta

* *Department of Information Engineering, University of Brescia, Via Branze 38, 25123 - Brescia, Italy (Tel: +39-030.3715449; e-mail: carneval@ing.unibs.it).*

Abstract: The air quality control is a challenging task, due to nonlinear processes that brings to pollution formation and accumulation in the troposphere. Control theory provides useful methodologies and tools to solve this problem. In this paper we propose a two-objective problem to control particulate matter exposure in the troposphere. The approach is based on the minimization of two objectives, namely the Air Quality Index and the emission abatement costs, depending on the decision variables (precursor emission reductions). In particular, this paper focuses on a novel source-receptor model structure able to describe the link between emission and concentration needed by the optimization procedure to describe the Air Quality Index. The methodology has been applied to Northern Italy, a region affected by PM_{10} levels, often exceeding the EU limit value established for health protection.

1. INTRODUCTION

The air quality control is a complex task, due to nonlinear formation and accumulation processes involving pollutants (mainly ozone and PM10) in the troposphere. In particular, concentrations of these pollutants are related to meteorological condition and to the emissions of the precursors, volatile organic compounds (VOC), nitrogen oxides (NO_x), ammonia (NH_3), primary particulate matter (PPM) and sulfur oxides (SO_x). Different techniques are available in literature to properly identify emission reductions, such as (a) scenario analysis (Lim et al. (2005)); (b) cost-benefit analysis (Reis et al. (2005), Schrooten et al. (2006)); (c) cost-effectiveness analysis (Schöpp et al. (1999), Amann et al. (2004)); (d) multi-objective optimization (Guariso et al. (2004), Carnevale et al. (2007)). The multi-objective approach allows calculating alternative optimal emission reduction strategies that consider the tradeoff among different targets, in this case the air quality improvement and the cost due to the implementation of a particular emission reduction policy. The multi-objective approach is not often applied in air quality control due to the difficulties to include in the optimization problem the non-linear dynamics involved in pollutants formation. In fact, the pollution-precursor relationship can not be simulated by deterministic 3D modeling systems, due to their high computational costs. So the identification of models capturing the relationship between the precursor emissions and secondary pollutant concentrations is required. For this purpose, source-receptor relationships have been implemented using isopleths (Flagen and Seinfeld (1988), Loughlin (1998)), and reduced form models such as (a) simplified models, adopting semi-empirical relations calibrated with experimental data as in Venkatram et al. (1994), or (b) statistical models, identified on the results of complex 3D transport-chemical model simulations as in Schöpp et al. (1999), Friedrich and Reis (2000), Guariso et al. (2004).

This work formalizes and applies a two-objective problem to select effective emission abatement strategies in the Po Valley. The optimization procedure is performed considering both (a) an air quality objective (the winter mean of PM_{10} concentrations), and (b) a cost objective (the costs due to the reduction of PM_{10} precursor emissions). The methodology proposes a source-receptor model able to describe the whole 3D domain and to estimate long term air quality indexes in a single simulation step, in contrast to previous works where different models for different cells were used (increasing the computational cost of the problem), and daily simulations were performed (Pisoni et al. (2009)). Such new approach allows the source-receptor models to handle more complex input patterns than the previous proposed one, in particular considering the prevalent wind direction over the area and its effects on PM10 concentrations.

2. PROBLEM FORMULATION

The decision model is formalized as a two-objective optimization problem, including the effectiveness of emission reduction policies on an Air Quality Index (AQI) and their costs (RC). The problem can be formalized as follows:

$$\min_{\theta} J(E(\theta)) = \min_{\theta}[AQI(E(\theta)) \quad RC(E(\theta))] \qquad (1)$$
$$\theta \in \Theta$$

where E represents the precursor emissions, θ are the decision variables, namely the emission reductions, constrained to assume values in Θ, $AQI(E(\theta))$ is the air quality objective and $RC(E(\theta))$ are the reduction costs, both depending on precursor emissions and emission reductions. In this section the formalization of the the control variables (2.1), the air quality (2.2) and the cost objectives (2.3) are presented. In particular, the methodology is applied to the case of particulate matter.

2.1 Control Variables

The control variables are defined as emission reductions in the so-called CORINAIR macrosector, a European classification based on the following 11 macrosectors (EMEP/CORINAIR, 1999):

(1) public power, cogeneration and district heating plants;
(2) commercial, institutional and residential combustion plants;
(3) industrial combustion;
(4) production processes;
(5) extraction and distribution of fossil fuels;
(6) solvent use;
(7) road transport;
(8) other mobile sources and machinery;
(9) waste treatment and disposal;
(10) agriculture;
(11) nature.

The control variables of the decision problem are the emission percent reductions $\theta = \left\{\theta^{p,s}\right\}_{s \in S}^{p \in P}$, for each PM precursor $p = \{VOC, NO_x, NH_3, PM, SO_x\}$ and CORINAIR macrosector s; so in principle there are 55 control variables (emission reductions).

2.2 Air quality objective

The full description of the relationship between PM and its precursors should be given by the application of deterministic 3D modeling systems; however these models are not of practical use in an optimization problem due to their high computational requirements. For this reason simplified source-receptor models have been identified through the processing of a limited number of simulations performed by a deterministic modeling system.

Air quality index The air quality index is defined as the PM_{10} exposure index over a grid domain and it is a function of emissions. The emissions are expressed with respect to a reference scenario and split into the CORINAIR macrosectors (EMEP/CORINAIR, 1999). Since a regional Authority can impose different reduction to different emission macrosectors, the air quality index (AQI) can be expressed stressing the emission dependence of the exposure index function (Ψ) for cell (i, j), as follows:

$$AQI(E(\theta)) = \Psi\left(E_{i,j}^{p,s}(\theta^{p,s})\right) \tag{2}$$

where $E_{i,j}^{p,s}$ is the emission of the p precursor species for macrosector s in the cell (i, j);

Deterministic approach PM10 concentrations are typically simulated by three-dimensional deterministic modeling systems. In this work the Gas Aerosol Modeling Evaluation System (GAMES) (Volta and Finzi, 2006) has been used. It consists of three main modules as shown in Figure 1: (a) the multi-phase Eulerian 3D model TCAM (Carnevale et al., 2008); (b) the meteorological pre-processor PROMETEO; (c) the emission processor POEM-PM (Carnevale et al., 2006). The general mass balance equation for a generic pollutant h, whose concen-

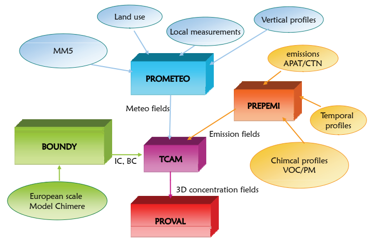

Fig. 1. The GAMES modeling system.

tration is C_h $[\mu g\ m^{-3}]$ (in spatial-temporal coordinates x, y, z, t), is then given by:

$$\frac{\partial C_h\,(x, y, z, t)}{\partial t} = T_h + R_h + D_h + S_h \qquad h = 1, 2, \ldots, n_{species} \tag{3}$$

where:

- T_h is the transport term $[\mu g\ m^{-3}\ s^{-1}]$;
- R_h is the reaction term $[\mu g\ m^{-3}\ s^{-1}]$;
- D_h is the deposition term $[\mu g\ m^{-3}\ s^{-1}]$;
- S_h is the source (emissions) term $[\mu g\ m^{-3}\ s^{-1}]$.

Equation 3 written for all considered species is the basis for the development of the air quality models. More details about the model can be found in Carnevale et al. (2008). Input and output of the deterministic model simulations are then used to identify source-receptor model, that implements the Air Quality Index in the optimization procedure. A daily simulation, performed over a three-dimensional domain of $64x41x11$ cells, takes 40 minutes of CPU times.

Source-receptor approach As previously stated, the function linking precursor emission levels to PM_{10} concentration has been here estimated through stochastic models formalized by means of neural networks, identified using deterministic model simulation scenarios (see Section 3.2 for more details). In particular, the feed-forward neural network (Figure 2) has been used in this study. This network computes a vector function $f_{NN} : \mathbb{R}^Q \rightarrow \mathbb{R}^L$ where Q and L are the dimensions of the net input and output vectors of the net respectively; the l-th element of the vector function f_{NN} is defined as (M is the number of the neurons in the hidden layer):

$$f_{NN}(v) = af_2\left(\sum_{m=1}^{M}(OW_{l,m} \cdot a_m) + g_l\right) \tag{4}$$

where:

$$a_m = af_1\left(\sum_{q=1}^{Q}(IW_{m,q} \cdot v_q) + b_m\right) \tag{5}$$

where af_1 and af_2 are real continuous functions, called activation function of the hidden layer (af_1) and of the output layer (af_2). The matrices IW ($M \times Q$) and OW ($L \times M$) are the input and output matrix respectively, and b ($M \times 1$) and g ($L \times 1$) vectors are the bias terms. Neural networks learn on a training data set, tuning the parameters IW, OW, b and g by means of a back-propagation algorithm.

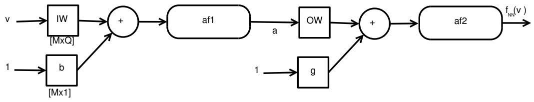

Fig. 2. Feed-forward neural network scheme.

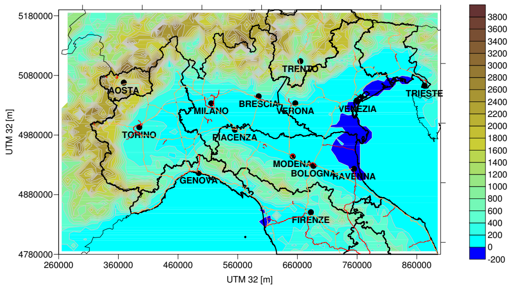

Fig. 3. Study domain (with orography and road network).

2.3 Cost objective

The cost objective of PM_{10} control can be formulated as follows:

$$RC(\theta) = \sum_p \sum_s RC^{p,s}\left(E^{p,s}(\theta^{p,s}), uc^{p,s}(\theta^{p,s})\right) \qquad (6)$$

where:

- $RC^{p,s}$ represents the total cost associated to reduction of precursor p in macrosector s;
- $E^{p,s}$ is the total annual emission of the p precursor species for macrosector s in the reference case;
- $uc^{p,s}$ represent the cost functions, that link emission reductions and unit cost, for each p precursor species and macrosector s.

The cost functions are polynomial cost curves, identified starting from the RAINS dataset (Amann et al., 2004) and encompassing all the technologies available to reduce pollutant emissions in every European country. More details about the methodology to derive cost objective are provided in Carnevale et al. (2007).

3. CASE STUDY

The methodology has been applied to Northern Italy (Figure 3), a region affected by PM_{10} levels often exceeding the EU limit value established for health protection. In particular, high concentrations characterize the central part of the domain, where the most important industrial and residential areas are located. A winter period (January 2004 - February 2004) has been selected for the simulation with the deterministic model, in order to only consider months with remarkable PM_{10} concentrations.

In the following subsections control variables selection (3.1), air quality objective (3.2) and cost objective (3.3), formalized in Section 2, will be presented for the selected case study.

3.1 Control variables

Control variables are the emission reductions for each CORINAIR macrosector. For PM_{10} in principle the problem should consider 55 control variables, eleven for each of PM_{10} precursor emission reductions, that is to say VOC, NO_x, NH_3, primary PM and SO_2. The optimization problem solution, however, does not consider the reduction of all the decision variables, due to the fact that in some CORINAIR macrosectors it is not possible to reduce emissions (i.e. biogenic emissions in macrosector 11 can not be abated), or there are no emissions on a particular macrosector. In Table 1, this information is summarized. $\Theta^{p,s}$ is the maximum feasible reductions allowed by the available technologies for pollutant p in the CORINAIR macrosector s (in the Table 1 'N.A'. means 'not applicable'). It is important to underline the case of macrosector 7 and 8. Technologies of these macrosectors can reduce at the same time VOC, PM and NO_x. To take into account this fact, in the optimization problem NO_x reductions are taken into consideration as decision variables, while VOC and PM emission reductions are constrained to NO_x ones using polynomial functions linking VOC to NO_x and PM to NO_x abatement efficiencies (Carnevale et al., 2007).

3.2 Air quality objective

The Air Quality Index, representing the value of PM_{10} concentration over the grid domain, has been evaluated through a source-receptor model based on a feed-forward neural network (Figure 2). Such network has been identified and validated by processing the results of the deterministic model TCAM, performed in the frame of Quitsat project (DiNicolantonio et al. (2009)). In particular, total emissions of NO_x, VOC, NH_3, primary PM and SO_2 have been used as input of the networks, and the corresponding average of PM_{10} as output. The datasets are referred to 11 scenarios: the basecase, assumed as the reference scenario, and 10 scenarios computed by reducing the precursors emissions. Table 2 presents the percentage of emissions reductions with respect to the Quitsat base case. Starting from these data, the target of the source-receptor models is to accurately estimate, for the whole domain, the winter average of pollutant given the precursors total emissions over the same period. One single neural network has been identified for the whole domain. This allows to speed up the whole procedure, without losing capability to reproduce local features (in fact even if there is a single neural network, its input change depending on the selected cell).

In more details, the output of the neural network are, for each domain cell, the PM10 concentration computed by TCAM model, while the input are the total precur-

Table 1. Maximum feasible reductions allowed by technologies, for PM_{10} precursors).

CORINAIR macros.	$\Theta^{VOC,s}$	$\Theta^{NO_x,s}$	$\Theta^{NH3,s}$	$\Theta^{PM,s}$	$\Theta^{SO_2,s}$
1	N.A.	0.76	N.A.	0.24	0.72
2	0.68	0.39	N.A.	0.59	0.56
3	N.A.	0.34	N.A.	0.09	0.60
4	0.19	0.80	N.A.	0.40	0.80
5	0.33	N.A.	N.A.	N.A.	N.A.
6	0.33	N.A.	N.A.	N.A.	N.A.
7	0.47	0.29	N.A.	0.41	0.76
8	0.06	0.25	N.A.	0.39	0.59
9	0.06	N.A.	N.A.	0.82	N.A.
10	N.A.	N.A.	0.58	N.A.	N.A.
11	N.A.	N.A.	N.A.	N.A.	N.A.

Table 2. Reductions applied to PM_{10} precursors emissions, with respect to Quitsat case base, for the 10 reduced emissions scenarios.

Scenario ID	NO_x	VOC	PM	SO_2	NH_3
1	30.89%	27.26%	21.45%	26.70%	35.85%
2	61.78%	54.52%	42.90%	53.40%	71.70%
3	61.78%	27.26%	21.45%	26.70%	35.85%
4	30.89%	54.52%	21.45%	26.70%	35.85%
5	30.89%	27.26%	42.90%	26.70%	35.85%
6	30.89%	27.26%	21.45%	53.40%	35.85%
7	30.89%	27.26%	21.45%	26.70%	71.70%
8	30.89%	54.52%	21.45%	53.40%	35.85%
9	61.78%	54.52%	21.45%	53.40%	71.70%
10	61.78%	27.26%	42.90%	26.70%	35.85%

Table 3. Identification and validation datasets sizes for the PM_{10} source-receptor model.

Feature	Value
Training	20 x 18304
Validation	20 x 2112

sors emission over 4 surrounding triangular-shaped zones, defined as described by Figure 5. The purpose of this configuration is to separately exploit (as input for the network) the information coming from 4 areas representative of the main wind directions. The N-S (North-South) direction is relevant due to the local breezes mountain-plain. The E-W (East-West) direction is the main wind direction over the domain. Consequently, 4 input for each precursor are required by the network to estimate the value of PM_{10} in each domain cell. In this work, a triangle height equal to 100 km has been selected. The main feature the corresponding neural network is summarized in Table 4.

A validation dataset has been selected by choosing approximately the 10% of the cells, distributed over the domain as shown in Figure 4. According to this, identification and validation datasets are characterized by the sizes reported in Table 3. Performances have been evaluated comparing the values of the AQI computed by the source-receptor model with the ones simulated by TCAM (as shown in Figure 6) providing good results. Statistical indexes computed for the validation dataset (Table 5) evidence how an accurate description of PM_{10} field is achieved.

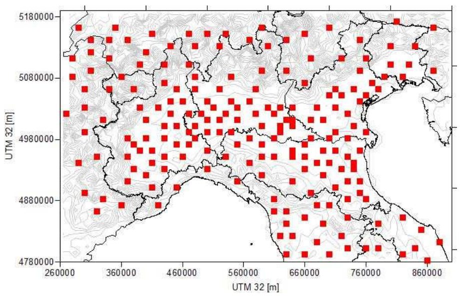

Fig. 4. Selected cells for the validation of the PM_{10} source-receptor model.

3.3 Cost objective

Abatement cost curves have been estimated on the basis of a large data set collected for Italy by IIASA (http://www.iiasa.ac.at). For each macrosector an emission abatement cost function has been estimated within

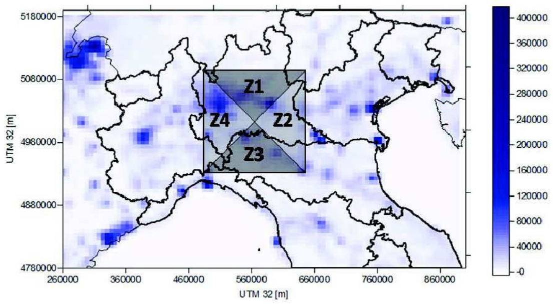

Fig. 5. Scheme representing, for a generic domain cell, the 4 areas (Z1, Z2, Z3, Z4) on which the emissions (ton/year) are considered as input of the Source-receptor model.

Table 4. Neural network structure of the PM_{10} source-receptor model.

Dataset	Pattern
No. neurons in the hidden layer (M)	20
Activation function hidden layer (af_1)	logsig
Activation function output layer (af_2)	purelin

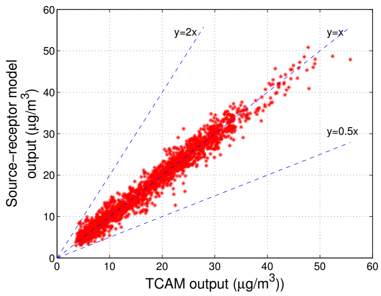

Fig. 6. Comparison between the values of the AQI simulated by TCAM and the ones computed by the source-receptor model

Table 5. Performance indexes of the neural network (NN) model computed for the validation dataset.

Index	Value
Mean NN model ($\mu g/m^3$)	17.59
Mean TCAM ($\mu g/m^3$)	17.63
Correlation	0.98
Mean error ($\mu g/m^3$)	-0.05
Absolute mean error ($\mu g/m^3$)	1.31
NMAE	0.07

zero and the maximum removal efficiency of technologies, with the constraint of identifying monotonically increasing and convex functions. Furthermore polynomial functions linking VOC to NO_x efficiency, and PM to NO_x efficiencies have been estimated, to update during optimization VOC and PM removal efficiency using NO_x removal efficiency of macrosector 7 and 8 (see Section 3.1). The cost function identification is described in Carnevale et al. (2007).

4. RESULTS AND DISCUSSION

The solutions of the multi-objective optimization problem application are shown in this Section. These results are obtained solving the multi-objective optimization problem by the weighted sum strategy. This means that an optimization problem is solved for different vector functions obtained as a linear combination of the 2 considered objectives (combined using a parameter α ranging between 0 and 1). These optimization problems are solved by means of the Sequential Quadratic Programming (SQP) method that performs, at each major iteration, an approximation of the Hessian of the Lagrangian function using a quasi-Newtonian method. This is then used to create QP subproblems, whose solution are used for a line search procedure (MathWorks, 2006). In Figure 7 the Pareto Boundary solution of the two-objective optimization approach is depicted. The Figure 7 shows in x-axis the total costs of implementation of emission reductions, and in y-axis represents the mean value of the Air Quality Index (mean PM10 concentration) computed for the 50% of the most polluted cells. The points of the Pareto Boundary present efficient solutions. As it is clear from the Figure, there is no single point solution of the problem, but a set of solution, representing the scale of values of the decision maker. In fact, possible solutions of the problem are both the no-reduction solution (point A, with a cost of 0 euro because no reductions are implemented, and with an Air Quality Index of 26 $\mu g/m3$), the maximum reduction solution (point C, with a cost of 450 Meuro, and an Air Quality Index of 15 $\mu g/m3$) and all the intermediate points (as i.e. point C). The Figure clearly communicates the maximum efficient cost that a decision maker can afford, and the maximum improvement of the Air Quality Index that can be obtained. The red diamond, in the right part of the Figure, represents the cost and Air Quality Index obtained implementing the Current LEgislation (CLE) planned by European Commission at 2020. This point represents the emissions level over the Domain at 2020, if the on-the-pipe European legislation will be implemented. This emission scenario is not a Pareto Efficient point for the study domain, characterized by strong nonlinearities in PM10 formation and accumulation.

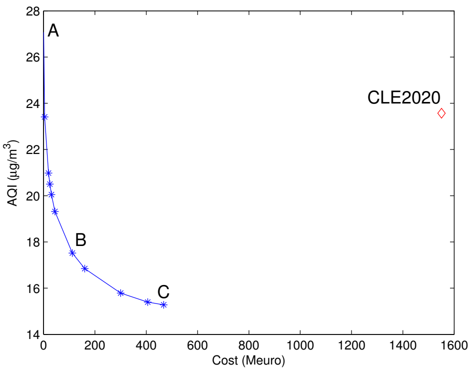

Fig. 7. Pareto boundary for the PM10 control problem (curve in blue) and Current LEgistlaion (CLE) projection point at 2020. The European Union emission projection at 2020, due to emission reduction legislation implementation, do not represent a Pareto efficient point for the study domain.

For each point of the Pareto boundary the two-objective problem also delivers the set of emission reductions (for precursor and pollutant) needed to obtain that particular results. As an example Figure 8 shows the emission reductions for PM, for the different macrosector, needed to obtain the points A, B and C depicted in Figure 7. The same kind of information, but for NOx, is shown in Figure 9.

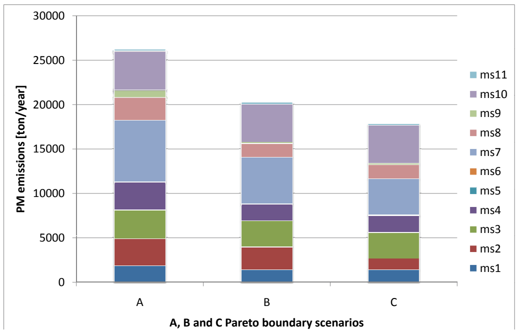

Fig. 8. PM Emission reductions for three points of the Pareto Boundary (point A, B, C). x axis represents the considered scenario, while y axis the ton/year of emissions to be reduced.

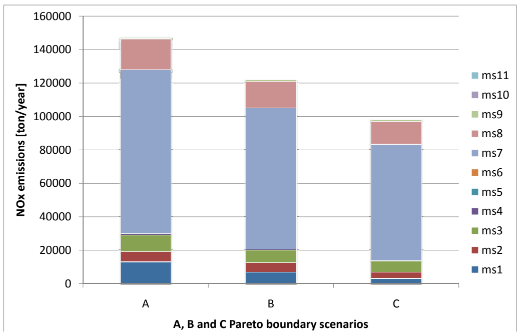

Fig. 9. NOx Emission reductions for three point of the Pareto Boundary (point A, B, C). x axis represents the considered scenario, while y axis the ton/year of emissions to be reduced.

Figure 10, Figure 11 and Figure 12 show, for the point A, B and C of the Pareto Boundary, the obtained results in terms of the Air Quality Index maps allowing to appreciate how the the Air Quality Index change spatially, choosing different policies from the Pareto Boundary.

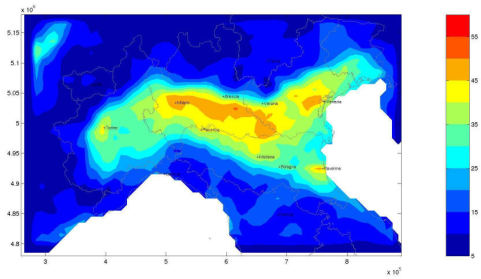

Fig. 10. Map of Air Quality Index ($\mu g/m3$) simulated for the no-reductions option.

5. CONCLUSIONS

In this work a two-objective optimization procedure has been presented, to control air quality (PM10 concentrations) at a regional level. The implemented methodology

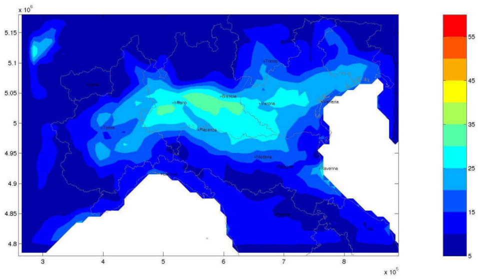

Fig. 11. Map of Air Quality Index ($\mu g/m3$) simulated for an intermediate option.

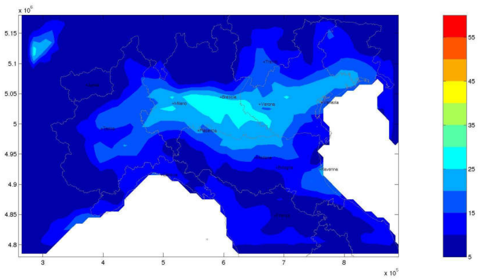

Fig. 12. Map of Air Quality Index ($\mu g/m3$) simulated for the maximum reductions option.

presents a new approach to identify source-receptor models used in the optimization procedure, based on neural network fed with emissions from zones representing prevalent wind directions over the domain. The data for the identification and validation of the neural network are provided by a deterministic chemical transport model, run over the same domain for different emission reduction scenarios. The validation of the source-receptor models identified using prevalent wind direction zones show good agreement in comparison to the deterministic model. Using these models the optimization problem has been solved, and results presented. The Pareto boundary shows the efficient solutions that a decision maker can implement, in terms of costs and Air Quality Index, and associated emission reductions.

6. ACKNOWLEDGMENTS

The work has been developed in the frame of EU NoE ACCENT (Atmospheric Sustainability). Part of this work has been also funded in the frame of Pilot Project QUITSAT (QUalita' dell'aria mediante l'Integrazione di misure da Terra, da SAtellite e di modellistica chimica multifase e di Trasporto - contract I/035/06/0 - http://www.quitsat.it), sponsored by the Italian Space Agency (ASI). We also acknowledge APD-IIASA staff for suggestions and data sharing.

REFERENCES

M. Amann, J. Cofala, C. Heyes, Z. Klimont, R. Mechler, M. Posch, and W. Schöopp. The RAINS model. Documentation of the model approach prepared for the RAINS peer review 2004. Technical report, International Institute for Applied Systems Analysis, 2004.

C. Carnevale, E. Decanini, and M. Volta. Design and validation of a multiphase 3D model to simulate tropospheric pollution. *Science of the Total Environment*, 390:166–175, 2008.

C. Carnevale, V. Gabusi, and M. Volta. POEM-PM: an emission model for secondary pollution control scenarios. *Environmental Modelling and Software*, 21:320–329, 2006.

C. Carnevale, E. Pisoni, and M. Volta. Selecting effective ozone exposure control policies solving a two-objective problem. *Ecological Modelling*, 204:93–103, 2007.

W. DiNicolantonio, A. Cacciari, A. Petritoli, C. Carnevale3, . Pisoni, M. L. Volta, P. Stocchi, G. Curci, E. Bolzacchini, L. Ferrero, C. Ananasso, and C. Tomasi. MODIS and OMI satellite observations supporting air quality monitoring. *Radiation Protection Dosimetry*, pages 1–8, 2009.

EMEP/CORINAIR. Atmospheric Emission Inventory Guidebook, second edition. Technical report, European Environment Agency, 1999.

R. C. Flagen and J. H. Seinfeld. *Fundamentals of Air Pollution Engineering*. Prentice-Hall Inc., 1988.

R. Friedrich and S. Reis. *Tropospheric ozone abatement*. Springer-Verlag, 2000.

G. Guariso, G. Pirovano, and M. Volta. Multi-objective analysis of ground-level ozone concentration control. *Journal of Environmental Management*, 71:25–33, 2004.

L. L. Lim, S. J. Hughes, and E. E. Hellawell. Integrated decision support system for urban air quality assessment. *Environmental Modelling & Software*, 20:947–954, 2005.

D. H. Loughlin. *Genetic algorithm-based optimization in the development of tropospheric ozone control strategies*. PhD thesis, Graduate Faculty of North Carolina State University, 1998.

MathWorks. Optimization Toolbox for Use with Matlab. Technical report, The MathWorks, 2006.

E. Pisoni, C. Carnevale, and M. Volta. Multi-criteria analysis for PM10 planning. *Atmospheric Environment*, 43:4833–4842, 2009.

S. Reis, S. Nitter, and R. Friedrich. Innovative approaches in integrated assessment modelling of European air pollution control strategies - Implications of dealing with multi-pollutant multi-effect problems. *Environmental Modelling & Software*, 20:1524–1531, 2005.

W. Schöpp, M. Amann, J. Cofala, C. Heyes, and Z. Klimont. Integrated assessment of European air pollution emission control strategies. *Environmental Modelling and Software*, 14:1–9., 1999.

L. Schrooten, I. De Vlieger, F. Lefebre, and R. Torfs. Costs and benefits of an enhanced reduction policy of particulate matter exhaust emissions from road traffic in Flanders. *Atmospheric Environment*, 40:904–912, 2006.

A. Venkatram, P. Karamchandani, P. Pai, and R. Goldstein. The development and application of a simplified ozone modeling system (SOMS). *Atmospheric Environment*, 28:3665–3678, 1994.

M. Volta and G. Finzi. GAMES, a comprehensive Gas Aerosol Modelling Evaluation System. *Environmental Modelling and Software*, 21:587–594, 2006.